Title

Heterologous Expression of the Mevalonic Acid Pathway in Cyanobacteria Enhances Endogenous Carbon Partitioning to Isoprene

Authors

Bentley, Fiona K
Zurbriggen, Andreas
Melis, Anastasios

Heterologous Expression of the Mevalonic Acid Pathway in Cyanobacteria Enhances Endogenous Carbon Partitioning to Isoprene

Fiona K. Bentley[2], Andreas Zurbriggen[2], and Anastasios Melis[1]

Department of Plant and Microbial Biology, University of California, 111 Koshland Hall, Berkeley, CA 94720-3102, USA

ABSTRACT   Heterologous expression of the isoprene synthase gene in the cyanobacterium *Synechocystis* PCC 6803 conferred upon these microorganisms the property of photosynthetic isoprene (C_5H_8) hydrocarbons production. Continuous production of isoprene from CO_2 and H_2O was achieved in the light, occurring via the endogenous methylerythritol-phosphate (MEP) pathway, in tandem with the growth of *Synechocystis.* This work addressed the issue of photosynthetic carbon partitioning between isoprene and biomass in *Synechocystis.* Evidence is presented to show heterologous genomic integration and cellular expression of the mevalonic acid (MVA) pathway genes in *Synechocystis* endowing a non-native pathway for carbon flux amplification to isopentenyl-diphosphate (IPP) and dimethylallyl-diphosphate (DMAPP) precursors of isoprene. Heterologous expression of the isoprene synthase in combination with the MVA pathway enzymes resulted in photosynthetic isoprene yield improvement by approximately 2.5-fold, compared with that measured in cyanobacteria transformed with the isoprene synthase gene only. These results suggest that the MVA pathway introduces a bypass in the flux of endogenous cellular substrate in *Synechocystis* to IPP and DMAPP, overcoming flux limitations of the native MEP pathway. The work employed a novel chromosomal integration and expression of synthetic gene operons in *Synechocystis*, comprising up to four genes under the control of a single promoter, and expressing three operons simultaneously. This is the first time an entire biosynthetic pathway with seven recombinant enzymes has been heterologously expressed in a photosynthetic microorganism. It constitutes contribution to the genetic engineering toolkit of photosynthetic microorganisms and a paradigm in the pursuit of photosynthetic approaches for the renewable generation of high-impact products.

Key words: biofuels; cyanobacteria; isoprene; isoprene synthase; metabolic engineering; photosynthesis; *Synechocystis*.

INTRODUCTION

Terpenoids are the largest family of naturally occurring products (more than 40 000 different molecules have been described) (Keeling and Bohlmann, 2012), and have diverse chemical properties that find application in the pharmaceutical, neutraceutical, cosmetic, and food industries (Bohlmann and Keeling, 2008). Terpenoids have potential to be also developed as biofuels (Lindberg et al., 2010; Peralta-Yahya et al., 2011). Accordingly, synthetic biologists have devoted considerable attention in recent years to the terpenoid biosynthetic pathways with the aim of increasing metabolic flux to ultimately increase terpenoid product yield in engineered microbes (Martin et al., 2003; Leonard et al., 2010; Zurbriggen et al., 2012; Bentley et al., 2013). One of the major challenges is the ability to experimentally control cellular carbon partitioning, in this case to channel a greater proportion of the endogenous substrate towards the terpenoid pathway without inducing negative consequences on cell fitness or

metabolism (Melis, 2013). Here, we report a genetic engineering strategy to increased photosynthetic carbon partitioning towards the terpenoid pathway in a cyanobacterial strain endowed with the ability to produce and release isoprene (C_5H_8) hydrocarbons (Lindberg et al., 2010; Bentley and Melis, 2012). This was achieved upon the heterologous expression of the mevalonic acid (MVA) pathway in *Synechocystis* sp. PCC 6803 (hereafter *Synechocystis*) to increase the pool of isopentenyl-diphosphate (IPP) and dimethylallyl-diphosphate

(DMAPP), the prenyl diphosphate precursors to isoprene and all other terpenoids.

There are two independent and distinct terpenoid biosynthetic pathways leading to the production of IPP and DMAPP (Figure 1). The methylerythritol-phosphate (MEP) pathway is of prokaryotic bacterial origin and present in most (but not all) bacteria, cyanobacteria, green microalgae, and plant plastids (Rohmer et al., 1996; Rohmer, 1999; Lange et al., 2000; Lichtenthaler, 2000; Lee and Schmidt-Dannert, 2002). The MEP pathway utilizes glyceraldehyde-3-phosphate (G3P) and pyruvate as primary feedstock molecules. The mevalonic acid (MVA) pathway is of archael/eukaryotic origin, and utilizes acetyl-CoA as the primary precursor (Miziorko, 2011). Most organisms also contain an IPP isomerase that catalyzes
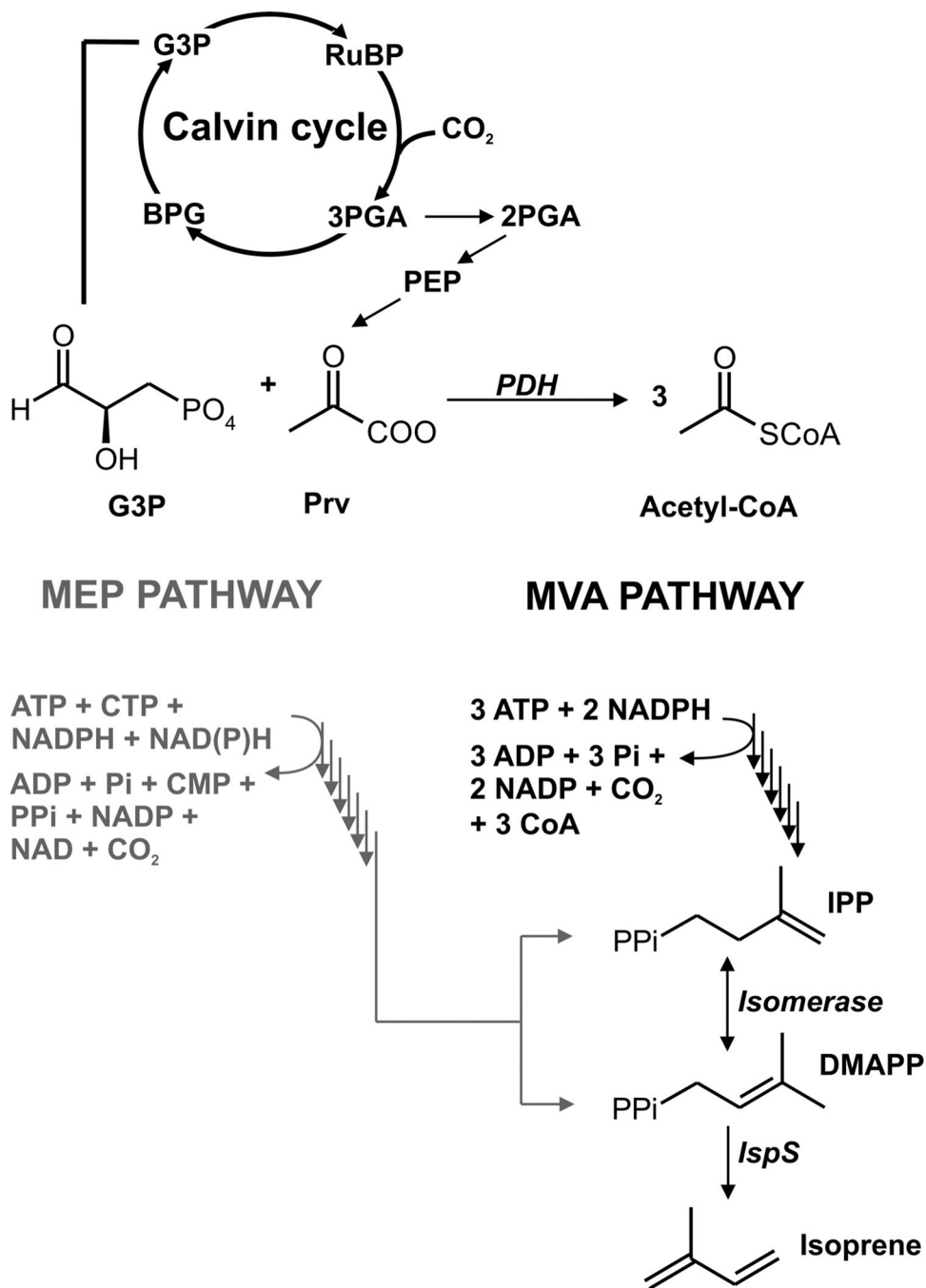

Figure 1. Photosynthetic Carbon Flux towards the Production of Isoprene.

G3P, glyceraldehyde-3-phosphate; RuBP, ribulose-1,5-bisphosphate; 3PGA, 3-phospho-glyceric acid; BPG, 1,3-biphosphoglycerate, 2PGA, 3-phospho-glycerate; PEP, phosphoenolpyruvate, Prv, pyruvate; PDH, pyruvate dehydrogenase; IPP, isopentenyl diphosphate; DMAPP, dimethylallyl diphosphate.

the inter-conversion of IPP and DMAPP. The native MEP pathway has been the target of genetic engineering efforts to increase the supply of IPP and DMAPP in *Escherichia coli* for increased synthesis of carotenoids and other terpenoid products (Kajiwara et al., 1997; Farmer and Liao, 2001; Kim and Keasling, 2001; Leonard et al., 2010; Zurbriggen et al., 2012). An alternative approach is to bypass the native MEP pathway

and its endogenous regulatory elements through the heterologous expression of the MVA pathway (Figure 2), which can operate in parallel with the MEP pathway, and, therefore, increase metabolic flux towards the intermediate metabolites IPP and DMAPP (Martin et al., 2003; Vadali et al., 2005; Yoon et al., 2009). Independent studies have shown that heterologous expression of the MVA pathway in non-photosynthetic
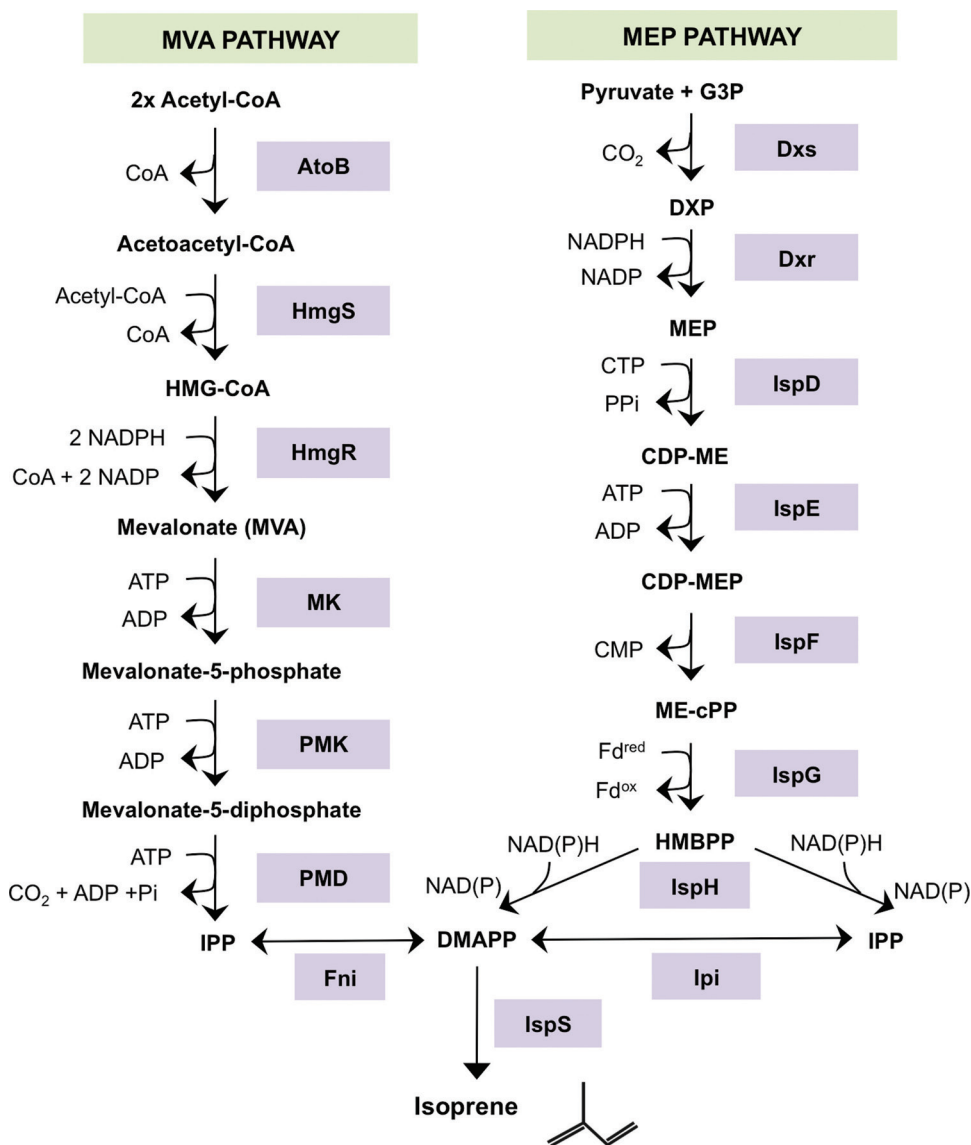

Figure 2. Comparative Endogenous Substrate Flux to IPP and DMAPP through the Mevalonic Acid (MVA) and Methylerythritol (MEP) Biosynthetic Pathways.

Genes of the MVA pathway in this study were derived from *E. faecalis*, *E. coli*, and *S. pneumoniae*. They were heterologolously expressed in *Synechocystis* sp. PCC 6803. Acetyl-CoA and pyruvate-G3P are the primary substrates for the MVA and MEP pathways, respectively, in both cases yielding isopentenyl diphosphate (IPP) and dimethylallyl diphosphate (DMAPP) as end products. The *P. montana* isoprene synthase (*IspS*) gene was optimized for codon usage in *Synechocystis* and heterologously expressed in this cyanobacterium to catalyze isoprene biosynthesis from DMAPP. MVA pathway enzymes: AtoB, acetyl-CoA acetyl transferase; HmgS, Hmg-CoA synthase; HmgR, Hmg-CoA reductase; MK, mevalonic acid kinase; PMK, mevalonic acid 5-phosphate kinase; PMD, mevalonic acid 5-diphoshate decarboxylase; Fni, IPP isomerase. MEP pathway enzymes: Dxs, deoxyxylulose 5-phosphate synthase; Dxr, deoxyxylulose 5-phosphate reductoisomerase; IspD, diphosphocytidylyl methylerythritol synthase; IspE, diphosphocytidylyl methylerythritol kinase; IspF, methyl erythritol-2,4-cyclodiphosphate synthase; IspG, hydroxymethylbutenyl diphosphate synthase; IspH, hydroxymethylbutenyl diphosphate reductase; Ipi, IPP isomerase; IspS, isoprene synthase.

systems increases terpenoid production to a much greater extent than supplemental expression of the native MEP pathway (Martin et al., 2003; Zurbriggen et al., 2012).

Photosynthetic microorganisms, such as cyanobacteria and microalgae, offer the advantage of high rates of photosynthesis and the potential to divert a greater proportion of photosynthetic resources to useful product than land plants (Melis, 2009). Moreover, they are better suited for the production and harvesting of volatile molecules, like isoprene, as they can be grown in fully enclosed photobioreactors suitable for product sequestration (Melis, 2012). Of current interest in the field is the issue of photosynthetic carbon partitioning between useful product and biomass (Melis, 2013), whereby the cell's own requirements and priorities for biomass generation are opposite to those of product generation. Work in this manuscript addressed the issue of altering photosynthetic carbon partitioning between isoprene and biomass in cyanobacteria upon the heterologous expression of a functional MVA pathway from *Enterococcus faecalis* and *Streptococcus pneumoniae* (bacteria possessing the MVA pathway) in *Synechocystis*. A successful heterologous expression of the yeast MVA pathway was recently reported in tobacco chloroplasts, aiming to enhance the production of isoprenoid metabolites in leaves (Kumar et al., 2012). In this work, two polycistronic MVA pathway constructs with genes derived from *E. faecalis*, *S. pneumoniae*, and *E. coli* (Zurbriggen et al., 2012) were expressed in *Synechocystis* that was previously engineered to express the isoprene synthase gene and to produce isoprene (C_5H_8) hydrocarbons (Lindberg et al., 2010; Bentley and Melis, 2012). An MVA pathway of bacterial origin was preferred in this case, as these have a better chance to be successfully expressed in cyanobacteria than MVA pathway from eukaryotic sources. Successful expression of each MVA operon and accumulation of the respective proteins in the soluble fraction of the *Synechocystis* cytosol is reported in this work. The rate and yield of isoprene production were elevated by approximately 2.5-fold in the transformant lines carrying the heterologous MVA pathway.

RESULTS

Construction of *Synechocystis* Strains Carrying the Heterologous MVA Pathway

Genes for the MVA pathway (Zurbriggen et al., 2012) were introduced to this *IspS* genetic background to see whether the addition of a second DMAPP-producing pathway increased the yield of the photosynthetically produced isoprene. The construction of strains carrying the *IspS* and MVA pathway genes was carried out in three sequential rounds of transformation.

Firstly, the codon-optimized isoprene synthase *IspS* gene from *Pueraria montana* (kudzu vine) (Sharkey et al., 2005) was introduced to a neutral site (*Neu*) in the *Synechocystis* wild-type genome via double homologous recombination

(Nagarajan et al., 2011). The *IspS* construct designed for integration at the *Neu* site included the native *Synechocysits psbA2* promoter, with the ribosomal binding site (RBS) and terminator for transcriptional control, a chloramphenicol-resistance selectable marker, and approximately 500 bp of upstream and 500 bp of downstream flanking sequence for allowing homologous recombination at the neutral site (Figure 3A). Importantly, the rate of isoprene production in this *IspS–ΔNeu* strain was the same as those measured in strains where the *IspS* gene was introduced to the *psbA2* site (Lindberg et al., 2010; Bentley and Melis, 2012).

The second round of transformation involved integration of the lower MVA pathway (encoding IPP isomerase (Fni), mevalonic acid kinase (MK), mevalonic acid 5-diphoshate decarboxylase (PMD), and mevalonic acid 5-phosphate kinase (PMK) from *S. pneumoniae*) at either of the *glgX* (a putative isoamylase-type debranching enzyme (slr0237)) or *glgA* (a glycogen synthase (sll0945)) sites of the *Synechocystis* genome. The genes were placed under the transcriptional control of the native *Synechocystis psbA2* promoter and terminator, and contained a spectinomycin-resistance selectable marker. The RBS within the *psbA2* promoter was utilized for Fni protein expression, whereas translation initiation regions (TIRs), consisting of RBSs and spacers, were cloned in front of each of the other genes. Approximately 500-bp upstream and downstream flanking sequences were included for targeting the constructs to either of the *glgX* or *glgA* sites.

The third round of transformation involved integration of the upper MVA pathway (encoding Hmg-CoA synthase (HmgS) and Hmg-CoA reductase (HmgR) from *E. faecalis* and acetyl-CoA acetyl transferase (AtoB) from *E. coli*) via homologous recombination at the *psbA2* site of the *Synechocystis* genome. The *E. faecalis* HmgR enzyme has both a thiolase activity and an HMGR-CoA reductase activity, and therefore catalyzes the first and third reactions of the MVA pathway. The AtoB-encoding gene from *E. coli* was also included in the upper MVA pathway construct as an extra thiolase in an effort to pull more acetyl-CoA towards the MVA pathway. The upper MVA construct included a kanamycin-resistance selectable marker, and was placed under the transcriptional control of the native *psbA2* promoter and terminator, which were included in the 500 bp of upstream (promoter) and 500 bp of downstream (terminator) of flanking sequence that targeted the construct to the *psbA2* site (Figure 3B). In this instance again, TIRs, consisting of RBSs and spacers, were cloned immediately upstream of each the HmgR- and AtoB-encoding open reading frames to allow protein translation from the polycistronic message, and the native RBS within the *psbA2* promoter was used for translation of HmgS.

Two different strains containing the heterologous MVA pathway genes were thus generated (termed MVA 1 and MVA 2), differing only in the site of genomic integration for the lower half of the MVA pathway (*glgX* or *glgA*, respectively). A number of different lines were isolated for each
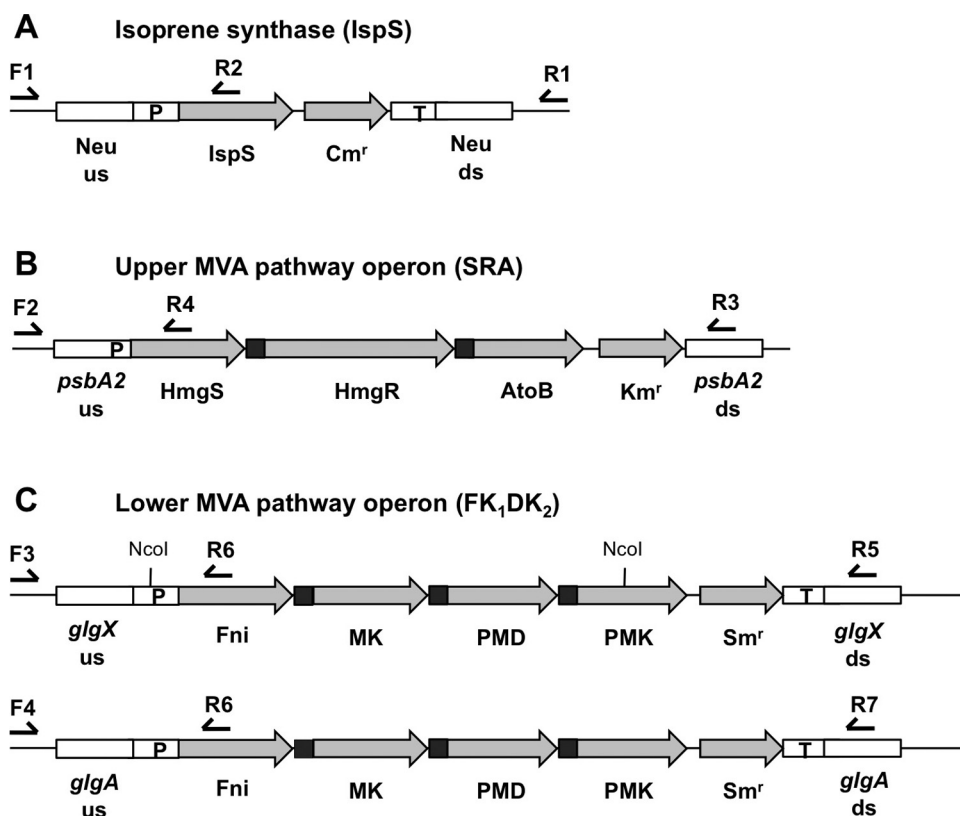
Figure 3. Constructs Designed for Expression of the Isoprene Synthase and the MVA Biosynthetic Pathway.

All transgenes were under the transcriptional control of the native *Synechocystis psbA2* promoter (P) and terminator (T) sequences. Translation initiation regions (TIRs), containing a ribosomal binding site and illustrated as black boxes, were placed in front of each MVA pathway gene, apart from those genes at the start of each operon, which used the native *Synechocystis* TIR of the *psbA2* gene within the upstream *psbA2* flanking region.

(A) The *P. montana* isoprene synthase gene (*IspS*) was codon-optimized for expression in *Synechocystis* and integrated within a neutral site (Neu) of the *Synechocystis* genome using the Neu flanking regions for homologous recombination. A chloramphenicol-resistance selectable marker (Cm^r) allowed for the selection of transformant lines.

(B) The upper MVA pathway operon (SRA) included genes encoding HmgS and HmgR from *E. faecalis* and AtoB from *E. coli*, and was cloned into the *psbA2* site of the *Synechocystis* genome using the *psbA2* flanking sequences for homologous recombination, and replacing the native *psbA2* gene. A kanamycin-resistance selectable marker (Km^r) allowed for the selection of transformant lines.

(C) The lower MVA pathway operon included genes encoding Fni, MK, PMD, and PMK from *S. pneumoniae*, and was cloned into the *glgX* or *glgA* site of the *Synechocystis* genome using the *glgX* and *glgA* flanking sequences, respectively, for homologous recombination. A spectinomycin-resistance selectable marker (Sm^r) allowed for the selection of transformant lines.

strain for assessment of isoprene production—that is, MVA 1.1, MVA 1.2, and MVA 1.3 represent independent lines of MVA 1, while MVA 2.1 and MVA 2.2 represent independent lines of MVA 2. A list of all strains used in this study is collated in Table 1.

The psbA2 promoter is a strong, light-sensitive promoter (Mohamed and Jansson, 1989), and was chosen to induce high expression levels of the heterologously expressed *IspS* gene and the MVA pathway genes in response to changes in irradiation intensity (Lindberg et al., 2010).

Verification of Genetic Transformation and Attainment of DNA Homoplasmy

Integration of the *IspS* and MVA pathway transgenes at targeted sites of the *Synechocystis* genome was implemented by double homologous recombination. Segregation of the *Synechocystis* DNA copies after each round of transformation was achieved upon cultivation of the transformants for several generations under antibiotic selective pressure. The selective pressure favors cell and the attendant DNA multiplication such that all new copies of the chromosome carry the selectable marker and transgenes—that is, conditions under which wild-type chromosomes do not propagate and are eventually lost. DNA copy homoplasmy was tested by genomic DNA PCR analysis with primers designed to the upstream and downstream regions of the targeted sites of integration (Figures 3 and 4). The stable incorporation of each transgene construct within the targeting sites of the genome was also verified by the use of primers designed to the coding regions of the first transgene in each synthetic construct (Figures 3 and 4).

Table 1. *Synechocystis* Strains Used in this Study.

Strain	Genotype	Description
WT	Wild-type *Synechocystis* sp. 6803	Wild-type genomic sequence
IspS	IspS–Δ*Neu*	Isoprene synthase gene inserted at the Neutral site (slr0168)
MVA 1	SRA–Δ*PsbA2*::FK$_1$DK$_2$–Δ*GlgX*::IspS–Δ*Neu*	Isoprene synthase gene inserted at the Neutral site (slr0168); upper MVA pathway (SRA) inserted at the *psbA2* site; lower MVA pathway (FK$_1$DK$_2$) inserted at the *glgX* site. MVA 1.1, MVA 1.2, and MVA 1.3 represent independent lines of the MVA 1 strain
MVA 2	SRA–Δ*PsbA2*::FK$_1$DK$_2$–Δ*GlgA*::IspS–Δ*Neu*	Isoprene synthase gene inserted at the Neutral site (slr0168); upper MVA pathway (SRA) inserted at the *psbA2* site; lower MVA pathway (FK$_1$DK$_2$) inserted at the *glgA* site. MVA 2.1 and MVA 2.2 represent independent lines of the MVA 2 strain
ΔGlgX	IspS–Δ*Neu*::Δ*GlgX*	Isoprene synthase gene inserted at the Neutral site (slr0168); *glgX* gene deleted. ΔGlgX 1, ΔGlgX 2, and ΔGlgX 3 represent independent lines of the ΔGlgX strain
ΔGlgA	IspS–Δ*Neu*::Δ*GlgA*	Isoprene synthase gene inserted at the Neutral site (slr0168); *glgA* gene deleted. ΔGlgA 1, ΔGlgA 2, and ΔGlgA 3 represent independent lines of the ΔGlgA strain

PCR amplification of genomic DNA with primers flanking the neutral site region, where *IspS* was integrated (primers F1/R1 in Figure 3A), generated a product of 1073 bp in the wild-type; however, this band was absent in all transformants carrying the *IspS* transgene, indicating that all wild-type copies of the neutral site DNA had been replaced by the *IspS* construct (Figure 4A). The presence of the *IspS* in these transformants was verified by the use of a reverse primer designed to the coding region of *IspS* (primers F1/R2, Figure 3A) to generate a product of expected size 935 bp, which was absent in the wild-type (Figure 4B).

Similar analyses were performed for the upper and lower MVA pathway transformations. Primers designed to amplify the *psbA2* site, which was used for integration of the upper MVA pathway (primers F2/R3, Figure 3B), generated a 1793-bp wild-type-sized band in the IspS strain, of which absence in the MVA transformants indicated homoplasmy for the introduced upper MVA pathway operon (Figure 4C). Amplification of the 1020-bp HmgS-encoding gene product (primers F2/R4, Figure 3C) in the MVA transformants confirmed the presence of the upper MVA pathway construct (Figure 4D). Likewise, amplification of the *glgX* and *glgA* regions, which were used for lower MVA pathway integration (primers F3/R5 and F4/R7, Figure 3C) generated wild-type-sized products of 3137 and 3124 bp, respectively, in the IspS strain, which were absent in the MVA transformants, indicating homoplasmy for the lower MVA operon (Figure 4E and 4F). Amplification of the 1251 and 1797-bp Fni-encoding gene products (primers F3/R6 and F4/R6, Figure 3C) in the MVA transformants

confirms the presence of the lower MVA pathway construct (Figure 4E and 4F).

Overall, these PCR analysis results indicated successful transformation of *Synechocystis* with the *IspS* and MVA pathway operon constructs, and, importantly, provided evidence of complete segregation of all transgene DNA copies, and elimination of all original wild-type DNA copies.

Expression of the *IspS* and MVA Pathway Transgenes

Transcription of the introduced *IspS* and MVA pathway transgenes in transformant lines was shown by RT–PCR (Figure 5), where primers were designed to amplify 200–300-bp amplicons from cDNA. The *IspS* amplicon was present in all transformants, confirming the expression of *IspS* mRNA. Similarly, amplicons for each of the MVA pathway genes (encoding HmgS, HmgR, AtoB, Fni, MK, PMD, and PMK) were present in all transformants carrying the heterologous MVA pathway. The Rubisco large subunit (*rbcL*) was amplified as a positive control and was present in all lines. No *rbcL* products were amplified in control samples that were prepared in the absence of reverse transcriptase, showing absence of genomic DNA contamination in all cDNA samples. These results confirmed that introduced *IspS* and MVA pathway transgenes were all expressed at the transcriptional level. Importantly, this also confirmed that the upper and lower MVA pathway operons were transcribed as a complete polycistronic message under the control of the *psbA2* promoter as evidenced by the presence of the terminal genes in each polycistron (encoding AtoB and PMK in the upper and lower MVA pathway operons, respectively).
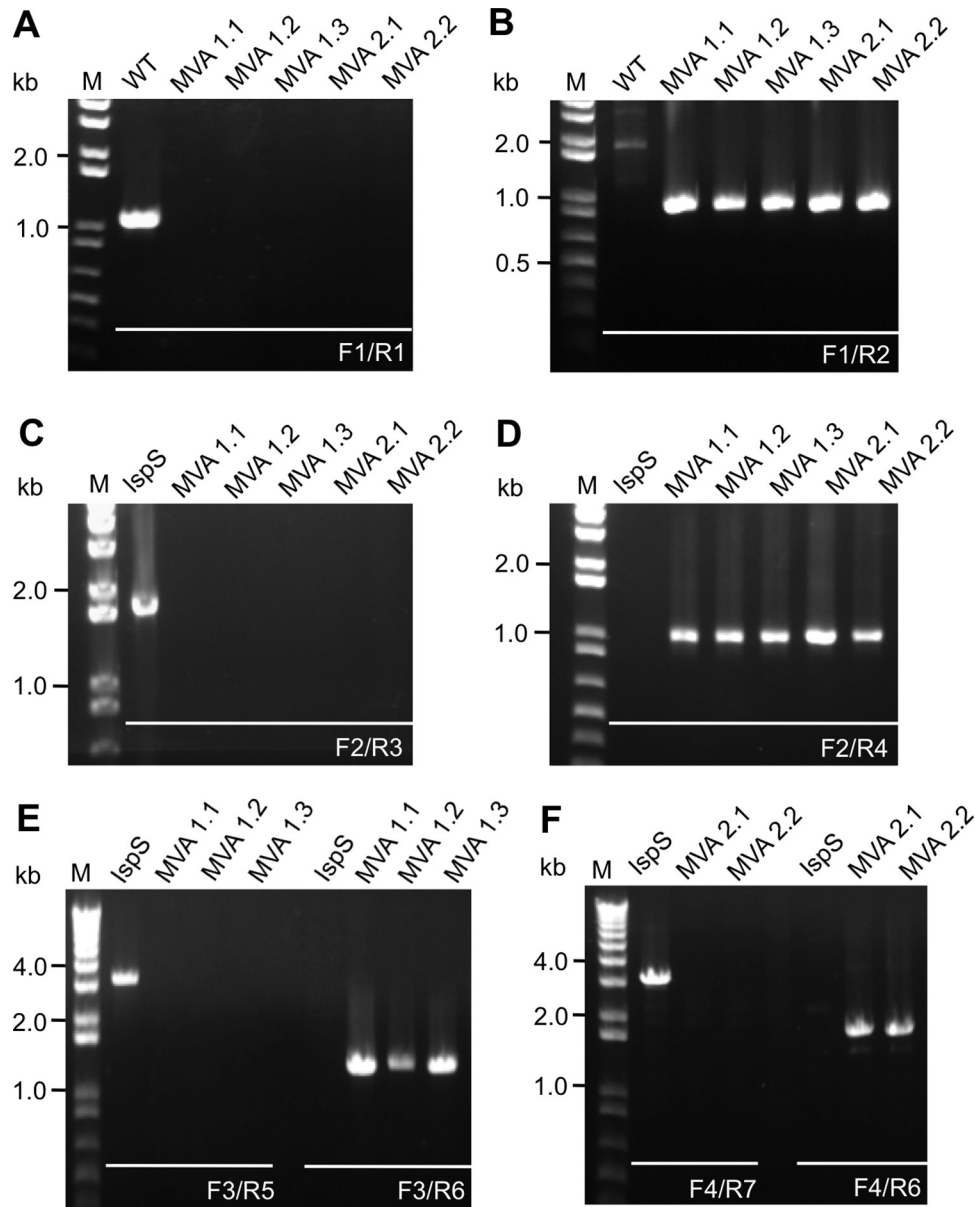
Figure 4. Test of Chromosomal Segregation for the Introduced Transgenes by Genomic DNA PCR Analysis.

MVA 1.1, MVA 1.2, and MVA 1.3 represent independent lines of the MVA 1 strain, while MVA 2.1 and MVA 2.2 represent independent lines of the MVA 2 strain.

(A) Primers upstream and downstream of the Neu site flanking regions used for homologous recombination (F1/R1 in Figure 3A) amplify the native 1073-bp Neu site region of the wild-type strain.

(B) Integration of the *IspS* gene within the Neu site in transformant lines was confirmed by using primers specific to the *IspS* gene (F1/R2 in Figure 3A) to amplify a 935-bp product.

(C) Primers designed to amplify the upstream and downstream *psbA2* flanking regions used for homologous recombination (F2/R3 in Figure 3B) resulted in a wild-type-sized 1793-bp product in the IspS strain.

(D) Integration of the upper MVA pathway operon (SRA) within the *psbA2* site is confirmed using primers specific to the HmgS-encoding gene (F2/R4 in Figure 3B) to amplify a 1020-bp product.

(E) Primers designed to amplify the upstream and downstream *glgX* flanking regions used for homologous recombination (F3/R5 in Figure 3C) resulted in a wild-type-sized 3137-bp product in the IspS strain. Integration of the lower MVA pathway operon (FK_1DK_2) within the *glgX* site is confirmed using primers specific to the Fni-encoding gene (F3/R6 in Figure 3C) to amplify a 1252-bp product.

(F) Primers designed to amplify the upstream and downstream *glgA* flanking regions used for homologous recombination (F4/R7 in Figure 3C) resulted in a wild-type-sized 3124-bp product in the IspS strain. Integration of the lower MVA pathway operon (FK_1DK_2) within the *glgA* site is confirmed using primers specific to the Fni-encoding gene (F4/R6 in Figure 3C) to amplify a 1797-bp product. All primer sequences are listed in Supplemental Table 3.
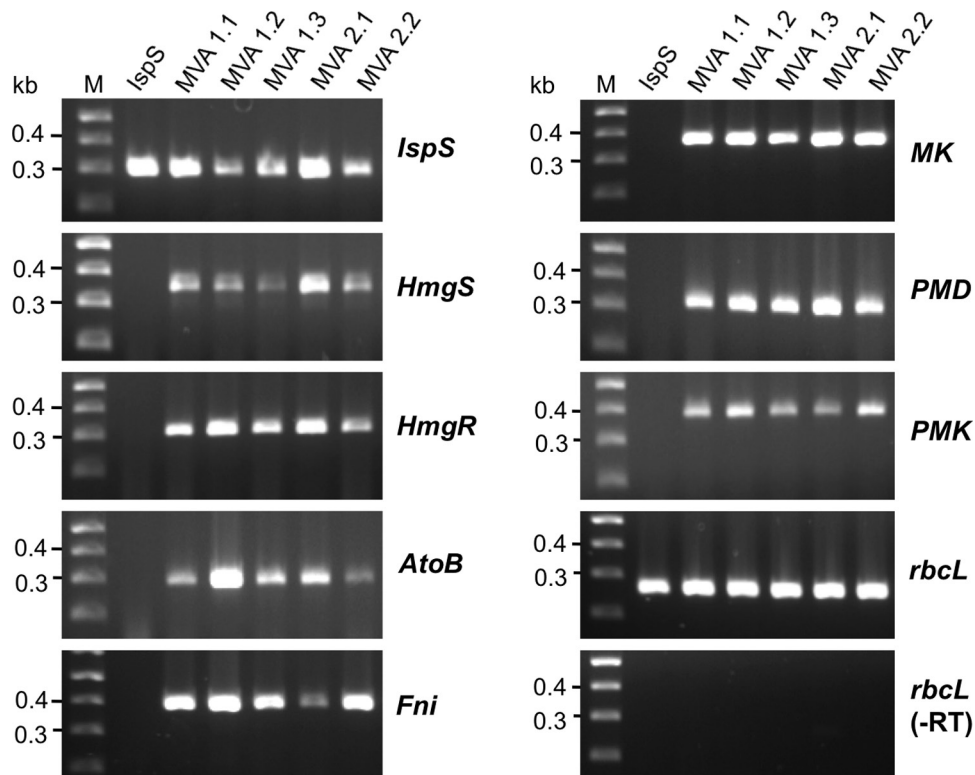
Figure 5. Transcription of the Recombinant MVA Pathway Genes as Shown by RT–PCR.

Primers designed to the coding regions of the recombinant *IspS* and MVA pathway genes (encoding HmgS, HmgR, AtoB, Fni, MK, PMD, and PMK) amplify PCR products from the cDNA samples of the five different MVA transformant lines (MVA 1.1, 1.2, 1.3, 2.1, and 2.2). The IspS recipient strain, which lacks the MVA pathway, is a negative control for MVA pathway gene expression. As a positive control, primers designed to the *rbcL* gene amplify a product in all lines. cDNA samples prepared in the absence of the reverse transcriptase (RT) enzyme do not yield products with the *rbcL* primers, indicating absence of DNA contamination in all samples.

Specific polyclonal antibodies were raised *de novo* against the *E. coli*-expressed recombinant IspS protein (Lindberg et al., 2010), and also for each of the MVA pathway recombinant proteins (HmgS, HmgR, AtoB, Fni, MK, PMD, and PMK) (Zurbriggen et al., 2012) and used to test for translation and presence of each of the recombinant proteins in transformant *Synechocystis* cells. The IspS protein has a predicted molecular weight of 65 kD, and the polyclonal IspS antibodies had a strong and specific cross-reaction to a protein of this size in the soluble fraction of cell extracts from all transformants (Figure 6). Similarly, the soluble fraction of cell extracts from MVA transformants provided strong cross-reactions to proteins of expected molecular weights for all of the MVA pathway recombinant proteins. The soluble extract from the IspS strain did not cross-react with any of the MVA pathway antibodies, confirming that the expression of the MVA pathway recombinant proteins is a result of the introduced MVA transgenes. Importantly, the successful expression of each MVA pathway protein indicated that RBSs cloned in front of each of the MVA pathway genes were effective in promoting ribosome binding at the beginning of each coding region of the polycistronic mRNA and initiation of translation. Detection of the recombinant proteins in the soluble fraction

of *Synechocystis* cell extracts indicated that these proteins all accumulate as soluble proteins within the *Synechocystis* cell.

Isoprene Production in Transformants Heterologously Expressing the MVA Pathway

The above results clearly showed that *Synechocystis* is amenable to stable incorporation and expression of the MVA pathway polycistronic gene constructs. Complete segregation was achieved for each of the heterologous constructs, and all transgenes were successfully expressed, leading to accumulation of each individual MVA pathway enzyme as a soluble protein in the *Synechocystis* cell. The major underlying question was whether the MVA pathway enzymes, if successfully expressed in *Synechocystis*, would be functionally active and capable of performing in an orchestrated manner to generate elevated amounts of IPP and DMAPP, and thereafter isoprene.

To test MVA pathway activity, isoprene production was measured in transformants carrying the *IspS* and MVA pathway transgenes, and compared with the strain carrying the *IspS* transgene only. Liquid cultures were grown under the conditions of the gaseous/aqueous two-phase bioreactor (Bentley and Melis, 2012), where 100% CO_2 gas slowly filled
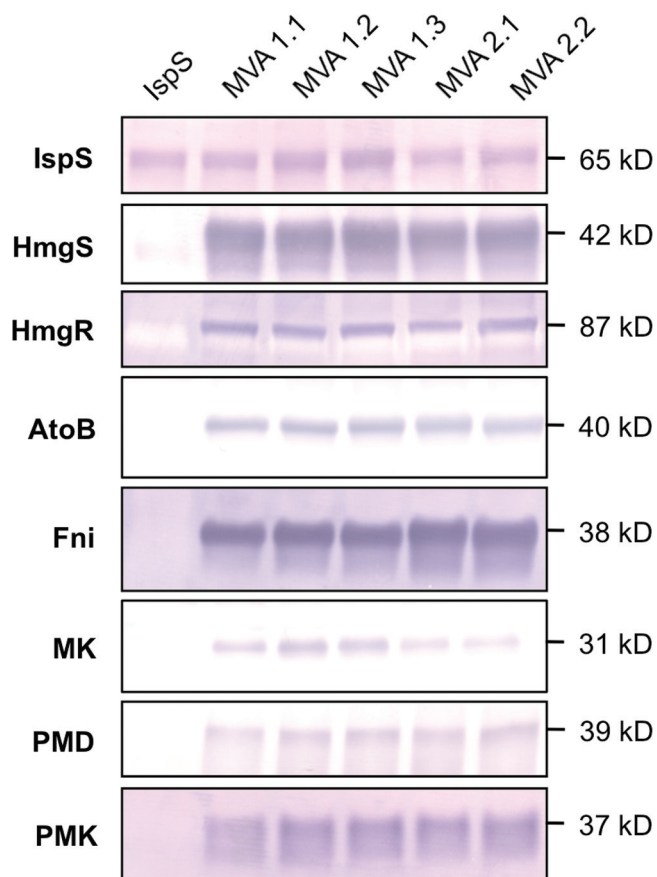
Figure 6. Immunodetection of the MVA Pathway Proteins in Transformant *Synechocystis* Cells.

The IspS recipient strain (left column), and the MVA1 and MVA2 strains (MVA 1.1, 1.2, 1.3, 2.1, and 2.2) were probed with specific polyclonal antibodies for IspS and the MVA pathway enzymes: HmgS, HmgR, AtoB, Fni, MK, PMD, and PMK. Each lane was loaded with 50 μg of soluble protein, which was obtained from the supernatant fraction of cells disrupted by French Press. The expected molecular masses for IspS and each protein of the MVA pathway are indicated.

the reactor headspace, before sealing the bioreactor to allow autotrophic biomass accumulation. Aliquots of 100% CO_2 were administered every 24 h to sustain high rates of biomass accumulation, which, under these conditions, doubled approximately every 24 h (Figure 7A). Cultures reached approximately 1 g of dry cell weight (DCW) per L culture over the 196-h experimental period. The rate of biomass accumulation in the MVA transformants was similar to that of the IspS strain, indicating that the expression of the MVA pathway did not adversely affect photoautotrophic growth (Figure 7A). Rates of isoprene production, however, were enhanced in the MVA transformants (Figure 7B).

Yield of isoprene production relative to biomass accumulation over the 196-h experimental period of photoautotrophic growth is shown in Figure 8. The IspS transformant produced around 120 μg isoprene g^{-1} DCW. Addition of the MVA pathway in the MVA transformants increased isoprene production

to about 250 μg isoprene g^{-1} DCW. The relative increase in the isoprene:biomass carbon partitioning ratio in the MVA transformants, compared with the IspS strain, was measured independently in multiple experiments and the averages of these are presented in Table 2. The MVA transformants consistently produced between 2.0- and 2.4-fold more isoprene on a biomass basis than the IspS strain, which did not carry the MVA pathway.

The above results showed that expression of the heterologous MVA pathway in *Synechocystis* carrying the *IspS* gene led to an enhancement of isoprene production by more than two-fold on a biomass basis, likely to be a result of increased carbon flux to IPP and DMAPP. The MVA pathway in this study enabled a minimum two-fold increase in the carbon partitioning of photosynthate towards the terpenoid biosynthetic pathway by providing an alternative route for the synthesis of DMAPP, the precursor of isoprene. The measured improvement in isoprene yield suggested that *IspS* enzymatic activity was limited by substrate availability in the IspS strain that lacks the MVA pathway.

Construction of Control Strains Carrying *glgX* and *glgA* Gene Deletions

The targeted integration of a heterologous gene to the chromosomal DNA of a host organism via homologous recombination requires that the chromosomal disruption itself is not the cause of associated phenotype, rather than the introduced transgene. The *psbA2* locus of the *Synechocystis* genome has been well established as a suitable site for transgene integration, as the deletion of the *psbA2* gene is compensated for by a strong up-regulation of the homologous *psbA3* gene (Mohamed et al., 1993). Accordingly, the *psbA2* site has been well utilized as a locus for transgene integration. The *Synechocystis* slr0168 locus has also been characterized as a 'neutral site' suitable for transgene integration (Nagarajan et al., 2011). The *psbA2* and 'neutral site' slr0168 loci were both used as sites for integration of transgene constructs in this study (for the upper MVA pathway construct and the *IspS* gene, respectively). Isoprene production and photoautotrophic growth was comparable in strains carrying the *IspS* gene in either the *psbA2* site (Lindberg et al., 2010) or the slr0168 'neutral site' (this study), indicating that the disruption of slr0168 itself did not cause any phenotypic effects under the experimental conditions used (results not shown). In this study, two additional chromosomal locations were utilized for integration of the lower MVA pathway construct, which have not previously been reported as 'neutral sites': the *glgX* and *glgA* loci. The *glgX* gene, slr0237 (encoding an isoamylase-type de-branching enzyme) and the *glgA* gene, sll0945 (encoding a glycogen synthase) both have two homologous genes in the *Synechocystis* genome. Recently, deletion of both *glgA* homologous genes was shown to inhibit glycogen biosynthesis in *Synechocystis*, whereas strains carrying a single deletion of either of the
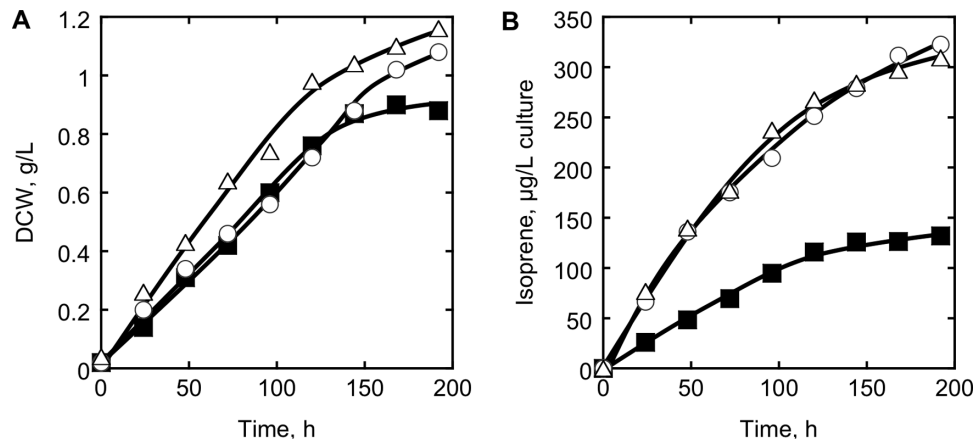
Figure 7. Time Course of Biomass Accumulation and Isoprene Production in Strains Carrying the Recombinant MVA Pathway.

Aliquots of 100% CO_2 were administered to the culture every 24 h to support photoautotrophic growth, after which the headspace of the biore-actor was sealed to allow for the accumulation of isoprene. Biomass accumulation as dry cell weight **(A)** and cumulative isoprene production **(B)** were measured over 196 h of photoautotrophic growth. Strains are: IspS (solid squares); MVA 1.1 (open circles); MVA 2.1 (open triangles). Results are representative of at least three independent experiments. Each of the five MVA pathway-containing lines produced similar results (MVA 1.1, 1.2, 1.3, 2.1, and 2.2).

glgA genes were indistinguishable from the wild-type (Grundel et al., 2012). It appears that, in many cases, when a gene has multiple isoforms, deletion of one homolog will be compensated for by the other isogene(s).

Control strains were constructed in this study that had gene deletions of *glgX* (slr0237) or *glgA* (sll0945) in the IpsS

Figure 8. Isoprene to Biomass Carbon Partitioning Ratio in Transformant Lines Carrying the Recombinant MVA Pathway.

Isoprene production is expressed as a proportion of biomass accumula-tion (dry cell weight) over 196 h of photoautotrophic growth in the IspS strain (lacking the MVA pathway) and five transformant MVA pathway-containing lines (MVA 1.1, 1.2, 1.3, 2.1, and 2.2).

parental strain to see whether these chromosomal disrup-tions had any influence on photoautotrophic metabolism or isoprene production under our experimental conditions. Multiple lines of the ΔGlgX and ΔGlgA strains were isolated—that is, ΔGlgX 1, ΔGlgX 2, and ΔGlgX 3 represent independent lines of ΔGlgX, while ΔGlgA 1, ΔGlgA 2, and ΔGlgA 3 repre-sent independent lines of ΔGlgA. Figure 9A and 9B show how ΔGlgX and ΔGlgA constructs were made, in which the *glgX* or *glgA* coding regions were replaced by a spectinomycin-resist-ance cassette. Following transformation of *Synechocystis*, the segregation of the *glgX* or *glgA* gene deletions was assessed by PCR. Primers designed to the up- and downstream *glgX* flanking regions used for homologous recombination (F3/R5 in Figure 9A) amplified a 3137-bp product in the IspS recipi-ent strain, and a smaller 2586-bp product in the ΔGlgX lines due to the deletion of the *glgX* gene (Figure 9C). Absence
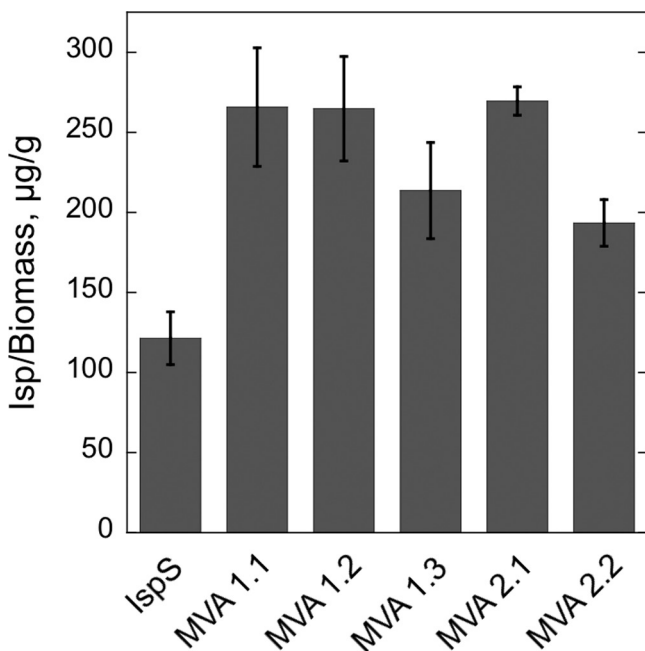
Table 2. Increase in the Isoprene:Biomass Carbon Partitioning Ratio upon Expression of the MVA Pathway in *Synechocystis*.

Strain	Isoprene:biomass ratio relative to that obtained with the IspS strain
MVA 1.1	2.3 ± 0.5
MVA 1.2	2.3 ± 0.3
MVA 1.3	2.4 ± 0.7
MVA 2.1	2.4 ± 0.3
MVA 2.2	2.0 ± 0.5

Increase shown is relative to the isoprene:biomass ratios measured in the *IspS* strain, which does not possess the MVA pathway. Measurements shown represent the average fold increase in isoprene:biomass ratios in at least three independent experiments, and the standard error of the mean is indicated. MVA 1.1, MVA 1.2, and MVA 1.3 represent inde-pendent lines of the MVA 1 strain, while MVA 2.1 and MVA 2.2 repre-sent independent lines of the MVA 2 strain.

of the parental 3137-bp amplicon in the ΔGlgX lines showed complete segregation for the gene deletion (Figure 9C). The primers designed to the up- and downstream *glgA* flanking regions used for homologous recombination (F5/R8 in Figure 9B) generated PCR products of similar size in the IspS recipient strain (1659 bp) and the ΔGlgA lines (1637 bp) (Figure 9D). Subsequent digestion of these PCR products with *Nae*I revealed the expected differential banding pattern in the IspS recipient strain and the ΔGlgA lines, showing successful deletion of the *glgA* gene (Figure 9E).

The results above confirmed the deletions of the *glgX* and *glgA* genes in the ΔGlgX and ΔGlgA strains, and that complete segregation for the gene deletions had been achieved. Rates of biomass accumulation in the ΔGlgX and ΔGlgA strains were similar to the IspS recipient strain, showing that these gene deletions did not have an adverse effect on photoautotrophic growth (Figure 10A). This was predicted because the MVA strains, which also have *glgX* or *glgA*

insertional deletions, also grew at a similar photoautotrophic rate to the IspS strain. Rates of isoprene production in the ΔGlgX and ΔGlgA strains were also measured to be similar to the IspS strain (Figure 10B). This result is significant because it confirms that the enhanced rate of isoprene production in the MVA pathway-containing strains is a direct result of the expression of the MVA genes, and that the associated *glgX* and *glgA* gene deletions are inconsequential in terms of isoprene production.

DISCUSSION

'Photosynthetic Biofuels' is a concept that envisions application of a single host organism acting both as photocatalyst and processor, generating ready-made fuels and offering a shortcut in the solar-to-biofuel production process (Lindberg et al., 2010; Melis, 2012). Photosynthetic microorganisms, such as cyanobacteria and green algae, are suitable host organisms, as
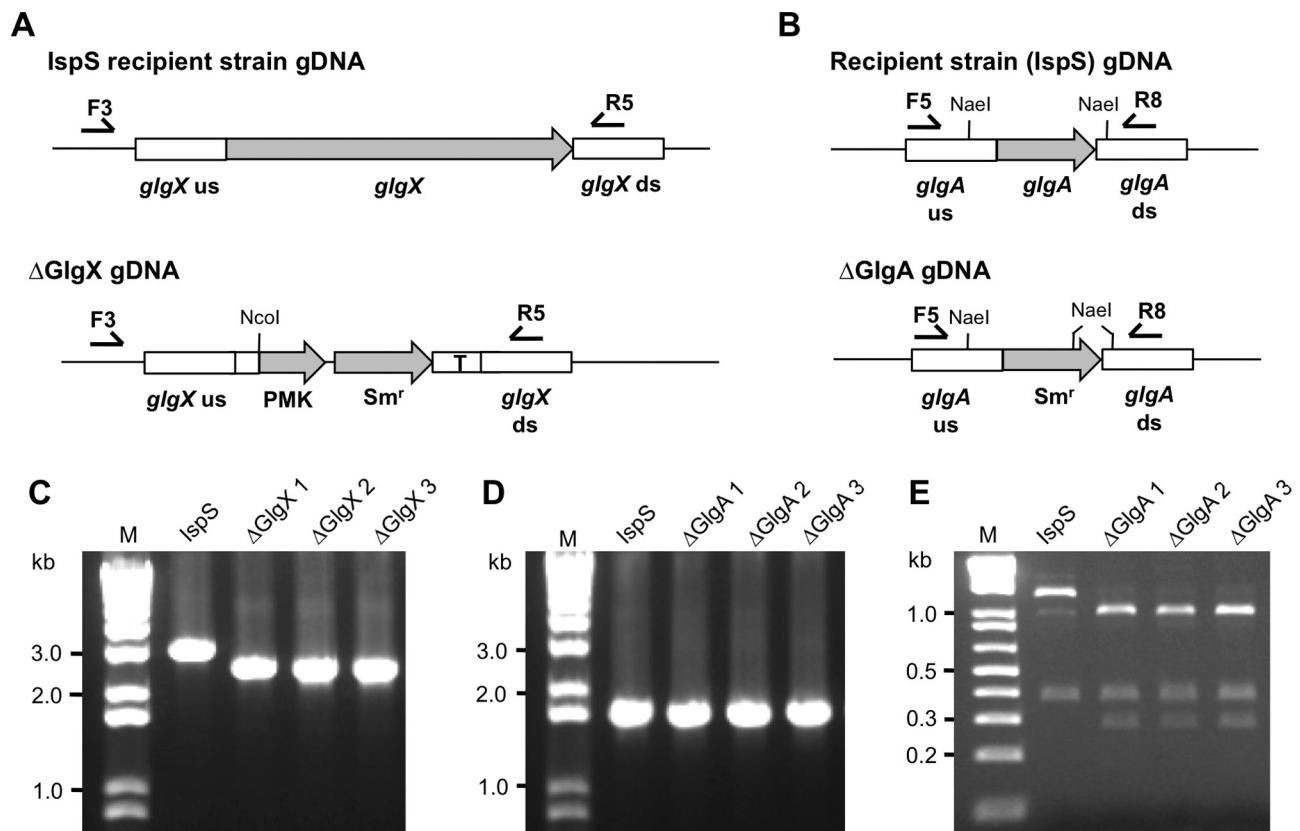

Figure 9. Construction and Analysis of Control Strains with *glgX* and *glgA* Gene Deletions.

The *glgX* **(A)** or *glgA* **(B)** genes were deleted in the IspS recipient strain through the replacement of the *glgX* or *glgA* gene ORFs with a spectinomycin-resistance cassette (Sm^r). The ΔGlgX strain contained a C-terminal portion of the PMK gene and the *psbA2* terminator (T), which were residual sequences from the plasmid used to integrate the lower MVA pathway (Fni, MK, PMD, and PMK) at the *glgX* site.

(C) Primers designed to amplify the upstream and downstream *glgX* flanking regions used for homologous recombination (F3/R5 in (A)) generated a 3137-bp product in the IspS recipient strain, and a 2586-bp product in the ΔGlgX lines (ΔGlgX 1, ΔGlgX 2, and ΔGlgX 3).

(D) Primers designed to amplify the upstream and downstream *glgA* flanking regions used for homologous recombination (F5/R8 in (B)) resulted in a 1659-bp product in the IspS recipient strain and a 1637-bp product in the ΔGlgA lines (ΔGlgA 1, ΔGlgA 2, and ΔGlgA 3).

(E) Digestion of these PCR products with *Nae*I revealed the expected sized band sizes of 1282 and 377 bp in the IspS recipient strain, and 977, 377, and 284 bp in the ΔGlgA lines. Primer sequences are listed in Supplemental Table 3.
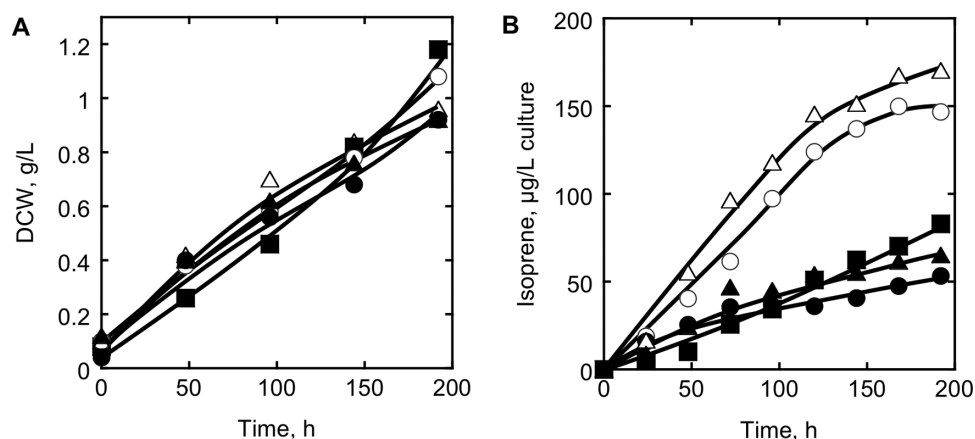
Figure 10. Biomass Accumulation and Isoprene Production in Control Strains with *glgX* or *glgA* Gene Deletions that Lack the Recombinant MVA Pathway.

Photoautotrophic growth was supported by aliquots of 100% CO_2 that were administered every 24 h, after which the headspace of the bioreactor was sealed to allow for the accumulation of isoprene. Biomass accumulation was measured as dry cell weight over 196 h of photoautotrophic growth **(A)** and the corresponding cumulative isoprene production was measured at similar time intervals **(B)**. Strains are: IspS (solid squares); MVA 1.1 (open circles); MVA 2.1 (open triangles); ΔGlgX 1 (closed circles); ΔGlgA 1 (closed triangles). Results are representative of at least three independent experiments. Similar results were observed with all other ΔGlgX and ΔGlgA lines.

they grow to high densities in sealed bioreactors (Chisti, 2007; Angermayr et al., 2009; Beer et al., 2009), and have better solar energy conversion efficiencies in photosynthesis than land plants (Melis, 2009). Cyanobacteria are amenable to transformation and expression of plant terpene synthases (Lindberg et al., 2010; Reinsvold et al., 2011; Bentley and Melis, 2012; Bentley et al., 2013), which catalyze the formation of terpenes with commercial value and the potential to be developed as fuels and chemicals. We have previously shown generation of isoprene hydrocarbons in a cyanobacterial system through the heterologous expression of the isoprene synthase (*IspS*) gene from *P. montana* (kudzu vine). Isoprene is a small, hydrophobic molecule that passes through cellular membranes, thereby separating from the biomass and accumulating as a volatile product in the headspace of a bioreactor, allowing for ease of harvesting (Bentley and Melis, 2012). Isoprene is a significant feedstock in the synthetic chemistry industry, where it is used to manufacture products ranging from rubber to adhesives and perfumes, and also has potential to be developed as a renewable fuel, where oligomerization of isoprene units may generate second-order fuel molecules to supplement gasoline, diesel, or jet fuel. For engineered photosynthetic microorganisms to be a viable source of isoprene, or any other terpene product, it is necessary to amplify carbon metabolic flux through the terpenoid biosynthetic pathway in order to achieve the desired product yields.

In non-photosynthetic prokaryotic microorganisms, such as *E. coli*, it is well established that introduction of a heterologous MVA pathway (to supplement the native MEP pathway) significantly boosts flux through the terpenoid pathway (Martin et al., 2003; Vadali et al., 2005; Yoon et al., 2009; Zurbriggen et al., 2012). Work from this lab recently achieved a more than 800-fold increase in isoprene production in *E. coli*

using this MVA-enhancement strategy. The heterologous expression of the MVA pathway circumvented the strong regulatory checkpoints of the native MEP pathway (e.g. the Dxs, Dxr, and Ipi enzymes; Kajiwara et al., 1997; Albrecht et al., 1999; Matthews and Wurtzel, 2000; Kim and Keasling, 2001), as the host microorganism does not possess the native MVA regulatory elements to attenuate flux through the MVA pathway. However, these promising results with *E. coli* were achieved in lab settings with high-copy plasmids operating in the cells. Expression of genes in the latter requires the presence of a selectable marker (typically antibiotics) to help retain the presence of the transgene-containing plasmids during cell growth. Use of antibiotics is not suitable for industrial production of isoprene, as large volumes, hence amounts of selectable marker, would be needed. To avoid this pitfall, transgenes need be stably incorporated in the cell's genomic DNA. After reaching DNA copy homoplasmy, the transformant cells can be used for industrial production without a need for the presence of any selectable markers.

Work in this manuscript demonstrated the first successful heterologous introduction of an entire biosynthetic pathway in the genomic DNA of a photosynthetic microorganism. The MVA pathway genes were divided into 'upper' and 'lower' polycistronic constructs for integration at two independent chromosomal locations in the *Synechocystis* genome. We showed stable integration of the two polycistronic constructs within the genomic DNA, followed by complete segregation for the introduced transgenes. The 'upper' MVA pathway was longer among the two polycistronic constructs, consisting of three genes of about 4.8 kb in length, while the 'lower' MVA pathway construct contained four genes of about 4.0 kb in length. Immunodetection of each of the MVA proteins in the soluble fraction of *Synechocystis* cell extracts indicated that the TIRs

(containing ribosome binding sites), which were introduced in front of each polycistronic gene, were effective in initiating protein translation. This is proof of concept that *Synechocystis* can express recombinant proteins from several polycistronic constructs. The approximately 2.5-fold increase in the rate of isoprene production in the *Synechocystis* strains carrying the *IspS* gene and the MVA pathway, compared with strains carrying only the *IspS* gene, demonstrated that each of the expressed MVA pathway enzymes was functionally active. Increase in isoprene production is likely to be a result of increased metabolic flux to the IPP and DMAPP isoprene precursors via the heterologous MVA pathway. Such enhancement in isoprene production suggested that, without an additional metabolite flux though the MVA pathway, activity of the IspS enzyme is limited by substrate availability. This understanding is significant because the MVA and MEP pathways utilize different substrates (acetyl-CoA for MVA, and G3P/pyruvate for MEP) to generate IPP and DMAPP. Addition of the MVA pathway provides the terpenoid pathway with another large cellular metabolite pool (acetyl-CoA) from which to draw carbon substrate.

Under conditions of saturating illumination, the function of an additional carbon sink in the form of isoprene that spontaneously diffuses away from the cells and the liquid culture could permit transformant cyanobacteria to assimilate CO_2 and photosynthesize with rates that are faster than those of the untransformed wild-type. Consistently with this notion, the measured improvement in isoprene yield has not occurred at the expense of biomass accumulation. In the particular case of our experiments, however, isoprene production rates are still slow relative to biomass accumulation to permit quantitative conclusions.

The proof-of-concept study described in this paper offers the stable genomic DNA integration of the MVA pathway in a photosynthetic microorganism and confirms functional activity of each individual heterologous enzyme. Further optimization of the process is required to ultimately improve isoprene production, beyond the 2.5-fold increase afforded here. In this respect, many studies have shown that multi-gene pathways require careful tuning of protein production in order to maximize titers (Alper et al., 2006; Pitera et al., 2007; Anthony et al., 2009), which can relieve bottlenecks, such as the HmgR (Pitera et al., 2007; Ma et al., 2011) and MK/PMK enzymes of the MVA pathway (Redding-Johanson et al., 2011). The ability to utilize the MVA pathway in photosynthetic microorganisms will pave the way for synthetic biologists to make substantial improvements in isoprenoid metabolism for the production of a diverse array of terpenoid products according to the direct photosynthesis-to-fuels concept.

METHODS

Cloning Procedures, Bacterial Strains, and Plasmids

The *E. coli* strain DH5α was used for routine sub-cloning and plasmid propagation, and grown in LB media with appropriate antibiotics at 37°C, according to standard protocols. Genomic DNA of *S. pneumoniae* (ATCC no. 6314), *E. faecalis* (strain V583; ATCC no. 700802), and *E. coli* were used as templates for PCR amplification of MVA pathway genes. The upper MVA pathway genes encoding HmgS (S) and HmgR (R) were cloned from *E. faecalis* and AtoB (A) from *E. coli*, and designated the 'upper' MVA pathway, while the lower MVA pathway genes encoding Fni (F), MK (K_1), PMD (D), and PMK (K_2) were cloned from *S. pneumonia* and designated the 'lower' MVA pathway. The isoprene synthase (*IspS*) gene from *P. montana* (Sharkey et al., 2005) (Genbank accession no. AY316691) was optimized for codon usage in *Synechocystis*, without the predicted chloroplast transit peptide, using the Gene Designer software (DNA 2.0, USA) (Lindberg et al., 2010). The oligonucleotide primers used to amplify these genes are listed in Supplemental Table 1, and show the positions of introduced restriction sites to aid cloning, as well as introduced TIR sequences in front of genes. The TIR sequence was composed of the RBS AGGAGG and spacer TAATAT (Zurbriggen et al., 2012).

Four regions of the *Synechocystis* genome were chosen as sites of integration for *IspS* and the two MVA pathway operons via double homologous recombination: (1) a neutral (Neu) site ORF (slr0168), encoding a hypothetical protein; (2) *psbA2* (slr1311), encoding the D1 protein; (3) *glgX* (slr0237), encoding a putative isoamylase-type debranching enzyme; and (4) *glgA* (sll0945), encoding a glycogen synthase. Oligonucleotide primers designed to amplify these regions, which were cloned into the pBluescript SK+ plasmid (Stratagene, USA), are listed in Supplemental Table 2. These regions are referred to as the upstream (us) and downstream (ds) flanking regions and equate to approximately 500 bp of sequence flanking either side of the transgene construct (Figure 2), and used for homologous recombination in *Synechocystis*.

The *IspS* transgene and a Cm^r selectable marker was inserted midway within the Neu site sequence, insertionally disrupting the slr0168 ORF, to create plasmid pIspS–Cm^r–ΔNeu. The upper MVA operon (SRA) along with a Km^r selectable marker were inserted between the up- and downstream flanking regions of *psbA2* to create plasmid pSRA–Km^r–ΔPsbA2. The lower MVA operon (FK$_1$DK$_2$) and the Sm^r selectable marker were inserted between the up- and downstream flanking regions of either *glgX* or *glgA* to create plasmids pFK$_1$DK$_2$–Sm^r–ΔGlgX and pFK$_1$DK$_2$–Sm^r–ΔGlgA, respectively. Promoter (P) and terminator (T) sequences, consisting of approximately 200 bp upstream (promoter) and 200 bp downstream (terminator) of the native *Synechocystis psbA2* ORF, were cloned immediately before and after the polycistronic transgene constructs (Figure 2), except for constructs with *psbA2* flanking regions that already contained these sequences.

In order to show that any phenotypes arising from the insertion of MVA transgenes into the *glgX* and *glgA* sites were not a direct result of *glgX* or *glgA* gene inactivation, control plasmids were designed to create ΔGlgX and ΔGlgA strains without MVA transgene integration. The plasmid

pSm^r–ΔGlgX was constructed by digesting pFK$_1$DK$_2$–Sm^r–ΔGlgX with *Nco*I (to remove most of the FK$_1$DK$_2$ lower MVA operon) and religated. The plasmid pSm^r–ΔGlgA was the parent plasmid of pFK$_1$DK$_2$–Sm^r–ΔGlgA, constructed prior to the insertion of the FK$_1$DK$_2$ lower MVA operon and the promoter/terminator sequences.

Cyanobacterial Strains, Growth Conditions, and Transformation Procedures

The glucose-tolerant cyanobacterial strain *Synechocystis* sp. PCC 6803 (Williams, 1988) was used as the recipient strain in this study, and is referred to as the wild-type. Wild-type and transformant strains were maintained on solid BG-11 media supplemented with 10 mM TES-NaOH (pH 8.2), 0.3% sodium thiosulfate, and 5 mM glucose. Where appropriate, kanamycin (Km) and spectinomycin (Sm) were used at a concentration of 25 μg ml^{-1}, and chloramphenicol (Cm) at 15 μg ml^{-1}. Liquid cultures were grown in the absence of antibiotics in BG-11 containing 25 mM sodium phosphate buffer, pH 7.5. Liquid cultures for inoculum purposes and for RNA or protein analyses were maintained at 25°C under a slow stream of constant aeration and illumination at 20 μmol photons m^{-2} s^{-1}. Growth conditions employed when measuring the production of isoprene from *Synechocystis* cultures are described below.

Transformation of *Synechocystis*, with the plasmid constructs described above, was performed according to established procedures (Eaton-Rye, 2011). Appropriate antibiotics were used for selection and maintenance of transformant strains on agar plate. Successful transgene incorporation and complete DNA cyanobacterial copy segregation for the introduced transgene constructs was verified by genomic DNA PCR, using primers listed in Supplemental Table 3. All strains used in this study are described in detail in Table 1.

Reverse-Transcription PCR

Cells were harvested in late-exponential growth phase for RNA isolation. Trizol reagent (Life Technologies) was used to extract total RNA from 25 ml of the liquid culture according to the manufacturer's instructions. Contaminating DNA was removed by treating the isolated RNA with DNase I (Life Technologies). cDNA was generated from 1 μg of RNA by reverse transcription using SuperScript III (Life Technologies). This was used as the template for PCR analysis, where gene-specific primers were used to amplify the transgenes, in addition to the *rbcL* gene as a positive control for transcription. These oligonucleotide primers are listed in Supplemental Table 4.

Western Blot Analyses

Cyanobacterial cells from liquid culture were harvested at late-exponential growth phase by centrifugation and re-suspended in a buffer solution containing 50 mM Tricine, 10 mM NaCl, 5 mM MgCl$_2$, and 100 μM PMSF. Cells were disrupted by French Press and then centrifuged to remove cellular debris. The supernatant was collected as the soluble protein fraction and the protein concentration was determined using the DC Protein Assay Kit (Bio-Rad, USA). Protein samples were separated by SDS–PAGE (Bio-Rad, USA) and then transferred to PVDF membrane for immunodetection using the rabbit immune serum containing specific polyclonal antibodies against IspS (Lindberg et al., 2010) and each of the MVA pathway proteins (Zurbriggen et al., 2012). Cross-reactions were visualized by the NBT/BCIP Alkaline Phosphatase Color Development assay (Bio-Rad, USA) according to the manufacturer's instructions.

Isoprene Production and Biomass Accumulation Assays

Synechocystis cultures for isoprene production assays were grown photoautotrophically in the absence of antibiotics in 1 L gaseous/aqueous two-phase photobioreactors, which are described in detail by Bentley and Melis (2012). Bioreactors were seeded with a 700-ml culture of *Synechocystis* cells at an OD$_{730}$ nm of between 0.2 and 0.3 in BG-11 medium containing 25 mM sodium phosphate buffer, pH 7.5. Inorganic carbon was delivered to the culture in the form of 500-ml aliquots of 100% CO$_2$ gas, which was slowly bubbled though the bottom of the liquid culture to fill the bioreactor headspace. Importantly, this quantity of CO$_2$ did not exceed the buffering capacity of the medium. Once atmospheric gases were replaced with 100% CO$_2$, the headspace of the bioreactor was sealed and the culture was incubated under continuous illumination of 150 μmol photons m^{-2} s^{-1} at 35°C. Slow continuous mechanical mixing was employed to keep cells in suspension and to promote balanced cell illumination and gaseous CO$_2$ diffusion into the liquid culture to support biomass accumulation. Uptake and assimilation of headspace CO$_2$ by cells were concomitantly exchanged for O$_2$ during photoautotrophic growth. The sealed bioreactor headspace allowed for the trapping, accumulation, and concentration of photosynthetically produced isoprene as a volatile product.

Gas from the headspace of sealed bioreactors was sampled and analyzed by gas chromatography using a Shimadzu 8A GC (Shimadzu, Columbia, MD, USA) equipped with a flame ionization detector (FID) and a Porapak N 80/100 column appropriate for detection of short-chain hydrocarbons. Quantitation of isoprene production was performed on the basis of an isoprene vapor calibration curve constructed by the GC analysis of a series dilution of a vaporized pure isoprene standard (Acros Organics, Fair Lawn, NJ, USA).

Cyanobacterial biomass accumulation was measured gravimetrically as DCW, where 5-ml samples of culture were filtered through 0.22-μm Millipore filters and the immobilized cells dried at 90°C for 6 h prior to weighing the DCW.

SUPPLEMENTARY DATA

Supplementary Data are available at *Molecular Plant Online.*

REFERENCES

Albrecht, M., Misawa, N., and Sandmann, G. (1999). Metabolic engineering of the terpenoid biosynthetic pathway of *Escherichia coli* for production of the carotenoids beta-carotene and zeaxanthin. Biotechnol. Lett. **21**, 791–795.

Alper, H., Fischer, C., Nevoigt, E., and Stephanopoulos, G. (2006). Tuning genetic control through promoter engineering. Proc. Natl Acad. Sci. U S A. **102**, 12678–12683.

Angermayr, S.A., Hellingwerf, K.J., Lindblad, P., and de Mattos, M.J.T. (2009). Energy biotechnology with cyanobacteria. Curr. Opin. Biotechnol. **20**, 257–263.

Anthony, J.R., Anthony, L.C., Nowroozi, F., Kwon, G., Newman, J.D., and Keasling, J.D. (2009). Optimization of the mevalonate-based isoprenoid biosynthetic pathway in *Escherichia coli* for production of the anti-malarial drug precursor amorpha-4,11-diene. Metab. Eng. **11**, 13–19.

Beer, L.L., Boyd, E.S., Peters, J.W., and Posewitz, M.C. (2009). Engineering algae for biohydrogen and biofuel production. Curr. Opin. Biotechnol. **20**, 264–271.

Bentley, F.K., and Melis, A. (2012). Diffusion-based process for carbon dioxide uptake and isoprene emission in gaseous/aqueous two-phase photobioreactors by photosynthetic microorganisms. Biotechnol. Bioeng. **109**, 100–109.

Bentley, F.K., García-Cerdán, J.G., and Chen, H.-C. (2013). Paradigm of monoterpene (β-phellandrene) hydrocarbons production via photosynthesis in cyanobacteria. BioEnergy Res. **6**, 917–929.

Bohlmann, J., and Keeling, C.I. (2008). Terpenoid biomaterials. Plant J. **54**, 656–669.

Chisti, Y. (2007). Biodiesel from microalgae. Biotechnol. Adv. **25**, 294–306.

Eaton-Rye, J.J. (2011). Construction of gene interruptions and gene deletions in the cyanobacterium *Synechocystis* sp. strain PCC 6803. Methods Mol. Biol. **684**, 295–312.

Farmer, W.R., and Liao, J.C. (2001). Precursor balancing for metabolic engineering of lycopene production in *Escherichia coli*. Biotechnol. Prog. **17**, 57–61.

Grundel, M., Scheunemann, R., Lockau, W., and Zilliges, Y. (2012). Impaired glycogen synthesis causes metabolic overflow reactions and affects stress responses in the cyanobacterium *Synechocystis* sp PCC 6803. Microbiology. **158**, 3032–3043.

Kajiwara, S., Fraser, P.D., Kondo, K., and Misawa, N. (1997). Expression of an exogenous isopentenyl diphosphate isomerase gene enhances isoprenoid biosynthesis in *Escherichia coli*. Biochem. J. **324**, 421–426.

Keeling, C.I., and Bohlmann, J. (2012). Plant Terpenoids, in Civjan, N. (ed.), Natural Products in Chemical Biology. New York: John Wiley & Sons, Inc. pp. 121–142.

Kim, S.W., and Keasling, J.D. (2001). Metabolic engineering of the nonmevalonate isopentenyl diphosphate synthesis pathway in *Escherichia coli* enhances lycopene production. Biotechnology and Bioengineering. **72**, 408–415.

Kumar, S., Hahn, F.M., Baidoo, E., Kahlon, T.S., Wood, D.F., McMahan, C.M., Cornish, K., Keasling, J.D., Daniell, H., and Whalen, M.C. (2012). Remodeling the isoprenoid pathway in tobacco by expressing the cytoplasmic mevalonate pathway in chloroplasts. Metab. Eng. **14**, 19–28.

Lange, B.M., Rujan, T., Martin, W., and Croteau, R. (2000). Isoprenoid biosynthesis: the evolution of two ancient and distinct pathways across genomes. Proc. Natl Acad. Sci. U S A. **97**, 13172–13177.

Lee, P.C., and Schmidt-Dannert, C. (2002). Metabolic engineering towards biotechnological production of carotenoids in microorganisms. Appl. Microbiol. Biotechnol. **60**, 1–11.

Leonard, E., Ajikumar, P.K., Thayer, K., Xiao, W.H., Mo, J.D., Tidor, B., Stephanopoulos, G., and Prather, K.L.J. (2010). Combining metabolic and protein engineering of a terpenoid biosynthetic pathway for overproduction and selectivity control. Proc. Natl Acad. Sci. U S A. **107**, 13654–13659.

Lichtenthaler, H.K. (2000). Sterols and isoprenoids. Biochem. Soc. Trans. **28**, 785–789.

Lindberg, P., Park, S., and Melis, A. (2010). Engineering a platform for photosynthetic isoprene production in cyanobacteria, using *Synechocystis* as the model organism. Metab. Eng. **12**, 70–79.

Ma, S.M., Garcia, D.E., Redding-Johanson, A.M., Friedland, G.D., Chan, R., Batth, T.S., Haliburton, J.R., Chivian, D., Keasling, J.D., Petzold, C.J., Lee, T.S., and Chhabra, S.R. (2011). Optimization of a heterologous mevalonate pathway through the use of variant HMG-CoA reductases. Metab. Eng. **13**, 588–597.

Martin, V.J.J., Pitera, D.J., Withers, S.T., Newman, J.D., and Keasling, J.D. (2003). Engineering a mevalonate pathway in *Escherichia coli* for production of terpenoids. Nat. Biotechnol. **21**, 796–802.

Matthews, P.D., and Wurtzel, E.T. (2000). Metabolic engineering of carotenoid accumulation in *Escherichia coli* by modulation of the isoprenoid precursor pool with expression of deoxyxylulose phosphate synthase. Appl. Microbiol. Biotechnol. **53**, 396–400.

Melis, A. (2009). Solar energy conversion efficiencies in photosynthesis: minimizing the chlorophyll antennae to maximize efficiency. Plant Sci. **177**, 272–280.

Melis, A. (2012). Photosynthesis-to-fuels: from sunlight to hydrogen, isoprene, and botryococcene production. Energy Environ. Sci. **5**, 5531–5539.

Melis, A. (2013). Carbon partitioning in photosynthesis. Curr. Opin. Chem. Biol. **17**, 453–456

Miziorko, H.M. (2011). Enzymes of the mevalonate pathway of isoprenoid biosynthesis. Arch. Biochem. Biophys. **505**, 131–143.

Mohamed, A., and Jansson, C. (1989). Influence of light on accumulation of photosynthesis-specific transcripts in the cyanobacterium *Synechocystis* 6803. Plant Mol. Biol. **13**, 693–700.

Mohamed, A., Eriksson, J., Osiewacz, H.D., and Jansson, C. (1993). Differential expression of the psbA genes in the cyanobacterium *Synechocystis* 6803. Mol. Gen. Genet. **238**, 161–168.

Nagarajan, A., Winter, R., Eaton-Rye, J., and Burnap, R. (2011). A synthetic DNA and fusion PCR approach to the ectopic expression of high levels of the D1 protein of photosystem II in *Synechocystis* sp PCC 6803. J. Photochem. Photobiol. B. **104**, 212–219.

Peralta-Yahya, P.P., Ouellet, M., Chan, R., Mukhopadhyay, A., Keasling, J.D., and Lee, T.S. (2011). Identification and microbial production of a terpene-based advanced biofuel. Nat. Commun. **2**.

Pitera, D.J., Paddon, C.J., Newman, J.D., and Keasling, J.D. (2007). Balancing a heterologous mevalonate pathway for improved isoprenoid production in *Escherichia coli*. Metab. Eng. **9**, 193–207.

Redding-Johanson, A.M., Batth, T.S., Chan, R., Krupa, R., Szmidt, H.L., Adams, P.D., Keasling, J.D., Lee, T.S., Mukhopadhyay, A., and Petzold, C.J. (2011). Targeted proteomics for metabolic pathway optimization: application to terpene production. Metab. Eng. **13**, 194–203.

Reinsvold, R.E., Jinkerson, R.E., Radakovits, R., Posewitz, M.C., and Basu, C. (2011). The production of the sesquiterpene β-caryophyllene in a transgenic strain of the cyanobacterium *Synechocystis*. J. Plant Physiol. **168**, 848–852.

Rohmer, M. (1999). The discovery of a mevalonate-independent pathway for isoprenoid biosynthesis in bacteria, algae and higher plants. Nat. Prod. Rep. **16**, 565–574.

Rohmer, M., Seemann, M., Horbach, S., BringerMeyer, S., and Sahm, H. (1996). Glyceraldehyde 3-phosphate and pyruvate as precursors of isoprenic units in an alternative non-mevalonate pathway for terpenoid biosynthesis. J. Am. Chem. Soc. **118**, 2564–2566.

Sharkey, T.D., Yeh, S., Wiberley, A.E., Falbel, T.G., Gong, D.M., and Fernandez, D.E. (2005). Evolution of the isoprene biosynthetic pathway in Kudzu. Plant Physiol. **137**, 700–712.

Vadali, R.V., Fu, Y.C., Bennett, G.N., and San, K.Y. (2005). Enhanced lycopene productivity by manipulation of carbon flow to isopentenyl diphosphate in *Escherichia coli*. Biotechnol. Prog. **21**, 1558–1561.

Williams, J.G.K. (1988). Construction of specific mutations in photosystem-II photosynthetic reaction center by genetic-engineering methods in *Synechocystis* 6803. Methods Enzymol. **167**, 766–778.

Yoon, S.H., Lee, S.H., Das, A., Ryu, H.K., Jang, H.J., Kim, J.Y., Oh, D.K., Keasling, J.D., and Kim, S.W. (2009). Combinatorial expression of bacterial whole mevalonate pathway for the production of beta-carotene in *E. coli*. J. Biotechnol. **140**, 218–226.

Zurbriggen, A., Kirst, H., and Melis, A. (2012). Isoprene production via the mevalonic acid pathway in *Escherichia coli* (bacteria). Bioenergy Res. **5**, 814–828.